*Iranian Journal of Operations Research*
Vol. 13, No. 1, 2022, pp. 83-102

# Stochastic Optimal Operation of a Multicarrier Energy System with Electric Vehicles and Combined Heat and Power Units

A. Malekijavan[1*], H. Zafarani[2], M. Aslinejad[3]

***Abstract:*** *The paper presents a scheme to supply energy consumers by using a multicarrier energy system (MES). Each MES unit consists of electrical vehicles (EVs), and combined heat and power (CHP) units, which are called energy hubs (EHs) hereinafter. The objective function minimizes the cost of energy of the whole system while considering power flow equations in electricity, heat, and gas grids, where constraints include technical index limits of MESs, EVs, and CHPs. The model has been formed as a non-linear problem (NLP), in the following, the present study proposes a linear programming (LP) model as a substitute for equations of the NLP method so that the global optimal solution is found with a low computation error. Furthermore, the demand parameters, electricity price, and characteristics of EVs are uncertain. To model these uncertainties, we adopt the point estimate approach. The case study of this research considers electricity, gas, and heating grids simultaneously. The energy hubs relate all three grids to each other. The method is tested on a system through simulation using GAMS software. According to obtained numerical results, the suggested LP approach reaches an optimal point with reduced computation time and low error compared to the original formulations. As a result, the indices of different networks are improved using power management of the energy hubs.*

***Keywords:*** *Combined heat and power systems, Electric vehicles, Linear programming, Multicarrier energy system, Point estimate method, Stochastic model.*

Manuscript was received on 03/06/2022, revised on 05/20/2022 and accepted for publication on 10/19/2022.

## NOMENCLATURE

Indices and sets:

| | |
|---|---|
| $e, g, h, t, l, k$ | Indices of buses in electrical, gas, and heating networks; time; linearization segments of piecewise method; and a circular constraint |
| $ref$ | Reference bus |
| $\phi_e, \phi_g, \phi_h, \phi_t, \phi_l, \phi_k$ | Sets of buses in electrical, gas, and heating networks; time; linearization segments of piecewise method; and circular constraints |

Variables: All variables are in per-unit (p.u.)

| | |
|---|---|
| $F^{gas}, F^{tem}, F^{p,ele}, F^{q,ele}$ | Flow of gas, heat, active and reactive power |
| $P^{Bat}, P^{loss}$ | Batteries' active power and chargers' power loss of EVs in the parking lot |
| $P^{CHP,ele}, P^{CHP,gas}, P^{CHP,tem}$ | Electrical, gas, and heating power of CHP |
| $P^{EV}, Q^{EV}$ | Active and reactive power of EVs in the parking lot |
| $P^{gas}, P^{tem}, P^{ele}$ | Station power in electrical, gas, and heating networks |
| $Q^{ele}, Q^{CHP,ele}$ | Station and CHP reactive powers |
| $T$ | Temperature |
| *Total cost* | Objective function value ($) |
| $V, \theta, \Delta V$ | Voltage magnitude, voltage angle (rad), and voltage deviation |

[1]Department of Electrical Engineering, University of Sattari, Tehran, Iran, amalekijavan@yahoo.com
[2]Department of Electrical Engineering, University of Kashan, Kashan, ha_zafarani@yahoo.com
[3]Department of Electrical Engineering, University of Sattari, Tehran, Iran, M.aslinezhad@ssau.ac.ir

| | |
|---|---|
| $\pi$, $\Delta\pi$ | Gas pressure and pressure deviation |

Parameters:

| | |
|---|---|
| $A^{ele}$, $A^{gas}$, $A^{tem}$ | Incidence matrices of buses and lines for electrical, natural gas, and district heating networks |
| $a^p$, $a^q$ | Power loss coefficients of chargers in the parking lot |
| $c$, $\dot{m}$ | Specific heat capacity of water, and mass flow rate of water |
| $CR^{max}$, $SE^{max}$ | Rate of charge of batteries and size of chargers in the parking lot (p.u.) |
| $EC$ | Required energy in the parking lot (p.u.) |
| $F^{e,max}$, $S^{max}$ | Maximum capacity of electrical line and generation (p.u.) |
| $D^{p,ele}$, $D^{q,ele}$, $D^{gas}$, $D^{tem}$ | Electrical (active and reactive power), gas and heating demands (p.u.) |
| $g$, $b$ | Conductance and susceptance (p.u.) |
| $P^{CHP,gmax}$, $P^{CHP,hmax}$, $S^{CHP,emax}$ | Maximum size of CHP in electricity, gas, and heating sectors (p.u.) |
| $P^{gas,max}$, $F^{g,max}$ | Maximum size of gas line and generation (p.u.) |
| $P^{tem,max}$, $F^{t,max}$ | Maximum size of heating line and generation (p.u.) |
| $T^{max}$, $T^{min}$ | Maximum and minimum temperatures (p.u.) |
| $V^{max}$, $V^{min}$ | Maximum and minimum voltages (p.u.) |
| $\rho^{ele}$, $\rho^{gas}$, $\rho^{tem}$ | Price of electrical, gas, and heat energies ($/MWh) |
| $\eta^{CHP}$, $\kappa$ | The efficiency of CHP, a pipeline constant (p.u.) |
| $\pi^{max}$, $\pi^{min}$ | Maximum and minimum pressures (p.u.) |

# I. INTRODUCTION

Management of multiple energies at the same is crucial for available energy resources like electrical, heat, and gas to name but a few, as well as modern technologies including CHP that are in connection with multiple types of energy [1]. Hence, an EH or an MES is introduced to help energy resources to be connected and converted into other types of energy, so that they can be stored for future use or transferred to other forms of energy [3]. Also, the management of MESs has more benefits than simply a single energy system management strategy [4]. Electric vehicles are an emerging technology that can connect to electrical networks to charge their batteries; they can replace gasoline cars [6]. It is noted that mismanagement of energy or power of EVs might result in their charging at electricity peak load time. Hence, the electricity demand at peak load hours increases. As a result, power loss and the voltage drop increase, and other challenges may also occur in the electrical network [7]. Therefore, EV energy management is a significant task to consider [10].

Numerous works have been carried out on MESs or energy hubs. In [11], a new large-scale NLP model was presented for power flow in an MES. In [12], the optimal power flow was presented for an EH with electricity and gas power inputs and electricity and heat power outputs. A multi-objective optimization was used to make energy costs minimized while taking into account operation and reliability indicators. Additionally, the paper discussed a probabilistic economic dispatch problem in an MES with wind turbines [13]. A bilevel problem model is presented in [14] for managing MES while taking into account network restructuring. Finally, based on these references, the MES management method was proposed as the NLP or mixed-integer NLP (MINLP). Different methods of evolutionary algorithms (EAs) such as modified teaching learning-based optimization (MTLBO) [15-16], genetic algorithm [11], time-varying acceleration coefficients, particle swarm optimization (TVAC-PSO) [17], and time-varying acceleration coefficient-gravitational search algorithm (SAL-TVAC-GSA) [18] are adopted to solve this formulation.

Different studies present energy or power management of EVs in parking lots. The authors in [19] refer energy and charging management of EVs, according to which EVs were charged at low electrical load hours for decreasing the charging cost. Charging/discharging power management was also presented

in [20]. According to this study, EVs were charged during medium and low electrical load periods and they were discharged during peak load time for decreasing energy cost and improving electrical network indices [21]. However, this strategy increased charging/discharging cycles and, consequently, decreased the lifetime of EV batteries [22]. Hence, the authors of [23], [24], and [25] discuss active and reactive power management of EVs where energy cost and voltage stability, and technical indicators are minimized. Several references have reported that, if an EV uses a bidirectional charger, it will be able to control the active and reactive power of the network in both directions, that is, from the network to the EV and vice versa [23]. Thereby, EVs can improve technical indices of electrical networks by injecting reactive power when needed [24]. Moreover, to decrease the cost of energy, the operators prefer to charge EVs during off-peak hours using active power control [23]. Since different parameters of EVs are uncertain, in [26], a robust model was presented for power management of EVs.

One approach to enhance the flexibility of microgrids is presented in [27], in which a bi-level multi-objective model, besides the power management system, is adopted. The suggested model takes into account the availability of renewable energy sources and flexibility-enhancing resources. These include a demand response program, storage equipment, and a combined system of electric spring and electric vehicle parking lot. The model, as mentioned, has two levels; the upper level finds the maximum profit of flexibility resources while considering its related limits. On the other hand, the lower level achieves the minimum cost of energy of microgrid and voltage deviation function by employing the Pareto optimization approach. Constraints are associated with linearized optimal AC power flow, renewable energy sources, flexibility limitations of the MG, and flexibility resources. A two-stage stochastic model is proposed in [28] to appropriately manage microgrids. The model takes into account the uncertainty variables associated with the output power of wind turbines, the demand, and the price of electricity. The model is in the form of a mixed-integer linear programming (MILP) problem. In another study, flexible power management (FPM) of networked microgrids is discussed when renewable energy sources and flexibility-enhancing resources are available in the system. Flexibility resources in this study consist of a new structure formed by integrating electric spring and electric vehicle parking lot with a demand response program. Ref. [30] focuses on a day-ahead EV scheduling so that unbalances in the system are reduced. To this end, the single-phase charging demand of EVs is controlled via vehicle to grid (V2G) power transfer. Moreover, the scheduling of electric vehicles is realized based on a demand response program based on electricity price. The authors in [31] coordinate the active and reactive power of distribution systems in which PVs are widely adopted. The proposed method helps reduce deviations of bus voltages, active power interruptions of PVs, and power loss, in addition to setting traditional voltage regulators such as on-load tap changers (OLTCs) and capacitor banks. Two separate levels are applied to find proper coordination between OLTC, capacitor banks, PVs, and battery energy storage systems.

As per the literature and taking a look at Table 1, most of the studies include EVs parking lot capability and models in electricity distribution systems, where the operation indicators like voltage profile and system power loss are improved using its active and reactive power control. But, based on [19], if EVs use the discharging operation to improve network indices, especially at peak load time, thus, the number of charging/discharging cycles in a day will be increased. Hence, the lifetime of EV battery will be decreased and this statement is not economic. Moreover, the reactive power control causes an increase in the switching number of EV chargers, where this statement can reduce the EV charger lifetime. Therefore, to cope with this issue, a suitable strategy is network management according to the coordination between EVs parking lots and distributed generations (DGs) to improve operation indices and increase EV battery and charger lifetime considering the works in [19-32]. Also, CHP is a suitable DG, which has higher energy efficiency than other DGs due to simultaneously generating heating and electricity energies. Therefore, the energy management problem of various power grids such as electricity, gas, and heating grids or MES management based on the coordination of EVs parking lot and

CHP is created in this condition to improve networks' operation indices and obtain high energy efficiency; this case has been less considered in the relevant literature. In addition, the MES management model is generally a large-scale non-convex NLP or MINLP according to [11] and more works such as [11] have used EA to solve this formulation. However, these solvers obtain the optimal solution at a high computational time and, generally, the optimal solution is not one in different solvers. To solve the challenge, the current study introduces an energy management model (refer to Figure 1) for different energy networks via the coordination of EVs and CHPs in EHs. Figure 1 shows that inputs to the MES are electricity and gas, while its outputs are electrical and heating energy. The MES also includes parking lots of EVs and CHPs, where active and reactive power is exchanged between EVs and electrical networks. CHPs receive gas power from gas networks and inject electrical and heat power into electricity and heat networks. The objective function attempts to make energy cost minimized in an MES. Constraints include the limitations of power flow equations and technical indices in MESs, EVs, and CHPs. It is noted that this formulation is similar to the NLP and the solution is to adopt an LP framework with the base formulation to reduce the computational time and obtain the global optimal solution. Additionally, electricity, gas, and heat power, price of electricity, and different parameters of EVs are uncertainties of the problem. Therefore, a stochastic model is utilized with the help of the point estimate method (PEM) so that uncertainties are modeled accurately. Eventually, the main innovations of the suggested approach are highlighted as follows:

- Adopting a coordination scheme for EVs parking lot and CHP in an EH to improve energy networks' operation indices and operation situation of EVs;
- Extracting the linearized optimal power flow model for the energy networks' operation problem including energy hub containing EVs parking lot and CHP,
- Employing the point estimate method to provide modeling of uncertainties, including energy demand from various types, price of energy, and EVs parameters using mean and standard deviation data; this method is suitable for MES problems that include more uncertain parameters than other scenario-based stochastic programming methods due to using low scenario samples and lack of need for scenario generation approaches.

**Table 1.** A summary of the literature

| Ref. No. | Problem model | | Solution method | Uncertainty | Non-MES model | | | MES model | | |
|---|---|---|---|---|---|---|---|---|---|---|
| | NLP | LP | | | DG | CHP | EV | DG | CHP | EV |
| [11-14] | Yes | No | EA | Yes | No | No | No | Yes | No | No |
| [15-16] | Yes | No | EA | No | No | No | No | Yes | Yes | No |
| [17-18] | Yes | No | EA | Yes | No | No | No | Yes | No | No |
| [19] | No | Yes | Simplex | No | No | No | Yes | No | No | No |
| [20-21] | Yes | No | CONOPT | Yes | No | No | Yes | No | No | No |
| [23] | No | Yes | Simplex | No | No | No | Yes | No | No | No |
| [24-25] | Yes | No | CONOPT | No | No | No | Yes | No | No | No |
| [26] | No | Yes | Simplex | Yes | No | No | Yes | No | No | No |
| [27-30] | No | Yes | Simplex | Yes | Yes | No | Yes | No | No | No |
| [31] | No | Yes | Simplex | Yes | Yes | No | No | No | No | No |
| [32] | No | Yes | Simplex | Yes | No | No | Yes | No | No | No |
| Proposed method | No | Yes | Simplex | Yes | No | No | No | No | Yes | Yes |

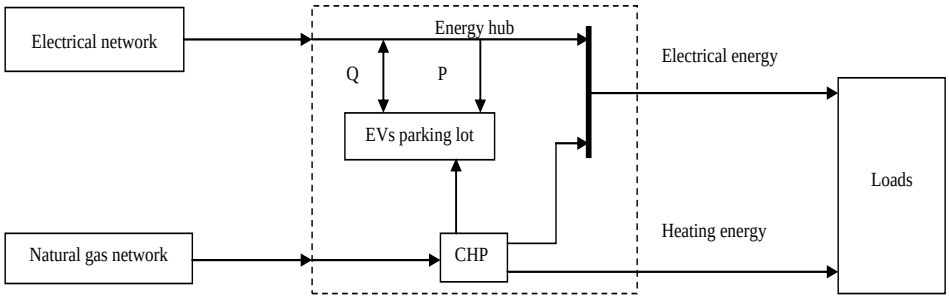


**Figure 1.** The proposed energy hub

The organization of the paper is described here. Section II describes the suggested NLP and LP models adopted for the MES management problem. Section III introduces uncertainties of the model using the PEM. Section IV presents simulation results obtained by applying the suggested method to case studies. Eventually, Section V gives a summary of the conclusions and innovations of the study.

# II. FORMULATION OF THE MODEL

## A. Original NLP problem

The original NLP problem is discussed here to minimize energy costs. Constraints include power flow equations and technical indicators concerning electricity, gas, and heat networks, EVs or parking lots, and CHP equations. Therefore, the formulation of the proposed problem can be expressed by the following steps:

1) Objective function: Equation ( 1 ) describes the objective function that minimizes the cost of energy in electricity, gas, and heat networks. The objective function has three terms; the first concerns the price of electricity received from an upstream network. The second and third terms introduce costs of gas and heating energy received from a gas station and a biomass (heating) station, respectively [16].

$$\min Total\cos t = \overbrace{\sum_{t\in\Phi_t}\sum_{e\in\Phi_e}\rho_t^{ele}P_{e,t}^{ele}}^{\text{Electrical energy cost}} + \overbrace{\sum_{t\in\Phi_t}\sum_{g\in\Phi_g}\rho^{gas}P_{g,t}^{gas}}^{\text{Gas energy cost}} + \overbrace{\sum_{t\in\Phi_t}\sum_{h\in\Phi_h}\rho^{tem}P_{h,t}^{tem}}^{\text{Heating energy cost}} \quad (1)$$

2) Power flow equations: This paper considers three networks, i.e. electricity, gas, and heat grids, power flow equations of which are represented by Equations ( 2 )-( 6 ). Equation ( 2 ) expresses the active power balance, and Equation ( 3 ) is the reactive power balance in the electrical buses at hour t. Equations ( 4 ) and ( 5 ) are active and reactive power flows, and Equation ( 6 ) is related to the angle of the voltage of the reference bus [25]. Constraints ( 7 ) and ( 8 ) state the power flow equation in the gas network. They introduce the power balance in gas nodes and the amount of gas in a pipeline at hour t, respectively [33]. The term sign($\pi_g$,$\pi_j$) is a function that is equal to 1 if $\pi_g$ is greater than $\pi_j$, and -1 if $\pi_j$ is greater than $\pi_g$ [33]. Equations ( 9 ) and ( 10 ) express the power balance in heat network nodes and the amount of heat passing through a pipeline, respectively [33]. $P^{ele}$, $Q^{ele}$, $P^{gas}$, and $P^{tem}$ are station power which is equal to zero in all the buses or nodes, except for the substation or reference bus.

$$P_{e,t}^{ele} + P_{e,t}^{CHP,ele} - D_{e,t}^{p,ele} - P_{e,t}^{EV} = \sum_{j \in \Phi_e} A_{e,j}^{ele} F_{e,j,t}^{p,ele} \quad \forall e,t \tag{2}$$

$$Q_{e,t}^{ele} + Q_{e,t}^{CHP,ele} - D_{e,t}^{q,ele} - Q_{e,t}^{EV} = \sum_{j \in \Phi_e} A_{e,j}^{ele} F_{e,j,t}^{q,ele} \quad \forall e,t \tag{3}$$

$$F_{e,j,t}^{p,ele} = g_{e,j}(V_{e,t})^2 - V_{e,t}V_{j,t}\begin{Bmatrix} g_{e,j}\cos(\theta_{e,t}-\theta_{j,t}) + \\ b_{e,j}\sin(\theta_{e,t}-\theta_{j,t}) \end{Bmatrix} \quad \forall e,j,t \tag{4}$$

$$F_{e,j,t}^{q,ele} = -b_{e,j}(V_{e,t})^2 + V_{e,t}V_{j,t}\begin{Bmatrix} b_{e,j}\cos(\theta_{e,t}-\theta_{j,t}) \\ -g_{e,j}\sin(\theta_{e,t}-\theta_{j,t}) \end{Bmatrix} \quad \forall e,j,t \tag{5}$$

$$\theta_{e,t} = 0 \quad \forall e = ref, t \tag{6}$$

$$P_{g,t}^{gas} - D_{g,t}^{gas} - P_{g,t}^{CHP,gas} = \sum_{j \in \Phi_g} A_{g,j}^{gas} F_{g,j,t}^{gas} \quad \forall g,t \tag{7}$$

$$F_{g,j,t}^{gas} = \kappa_{g,j} sign(\pi_{g,t}, \pi_{j,t}) \sqrt{sign(\pi_{g,t}, \pi_{j,t})(\pi_{g,t}^2 - \pi_{j,t}^2)} \quad \forall g,j,t \tag{8}$$

$$P_{h,t}^{tem} + P_{h,t}^{CHP,tem} - D_{h,t}^{tem} = \sum_{j \in \Phi_h} A_{h,j}^{tem} F_{h,j,t}^{tem} \quad \forall h,t \tag{9}$$

$$F_{h,j,t}^{tem} = c_{h,j}\dot{m}_{h,j}(T_{h,t} - T_{j,t}) \quad \forall h,j,t \tag{10}$$

3) CHP constraints: The input power to CHP is gas power, while the output power has two forms including electrical and heating power. CHP constraints are stated by Equations ( 11 ) through ( 14 ). These equations express the power balance between the electricity, gas, and district heating sectors of CHP ( 11 ) as well as the limit of natural gas ( 12 ), electrical ( 13 ), and district heating parts ( 14 ) in CHP [33]. Also, the CHP placement in the electrical, gas, and heating networks is specified by indices *e*, *g*, and *h*, respectively.

$$P_{g,t}^{CHP,gas} = \frac{1}{\eta^{CHP}}(P_{e,t}^{CHP,ele} + P_{g,t}^{CHP,tem}) \quad \forall e,g,h,t \tag{11}$$

$$0 \le P_{g,t}^{CHP,gas} \le P_g^{CHP,g\max} \quad \forall g,t \tag{12}$$

$$(P_{e,t}^{CHP,ele})^2 + (Q_{e,t}^{CHP,ele})^2 \le (S_e^{CHP,e\max})^2 \quad \forall e,t \tag{13}$$

$$0 \le P_{h,t}^{CHP,tem} \le P_h^{CHP,h\max} \quad \forall h,t \tag{14}$$

4) Parking lot (EVs) constraints: In this study, it is considered that 1) EVs in parking lots are connected to the network, 2) EVs are charged to supply the energy need of a day once arriving at the parking lot [23], and 3) EVs are operated in both charging-capacitive and charging-inductive modes, but not in discharging mode. Based on [23], as the number of charge and discharge cycles of the battery increases, the battery's lifespan shortens. As a result, EV owners prevent from procuring active power to the network. Therefore, the constraints of this section are as follows:

$$P_{e,t}^{EV} = P_{e,t}^{Bat} + P_{e,t}^{loss} \quad \forall e,t \tag{15}$$

$$P_{e,t}^{loss} = a^p \left|P_{e,t}^{EV}\right| + a^q \left|Q_{e,t}^{EV}\right| \quad \forall e,t \tag{16}$$

$$0 \le P_{e,t}^{Bat} \le CR_{e,t}^{\max} \quad \forall e,t \tag{17}$$

$$(P_{e,t}^{EV})^2 + (Q_{e,t}^{EV})^2 \le (SE_{e,t}^{\max})^2 \quad \forall e,t \tag{18}$$

$$\sum_{t \in \Phi_t} P_{e,t}^{Bat} = EC_e \quad \forall e \tag{19}$$

Equation ( 15 ) expresses the power balance between the electrical network and EVs batteries for a parking lot on bus *e*. The power loss of EVs or all chargers of EVs is expressed by Equation ( 16 ). The equivalent charge rate for all EV batteries is stated by Equation ( 17 ). It is noted that the term $CR^{max}$ is

equal to $CR_t^{\max} = \sum_{i=1}^{NE_t} CR_i$, where *CR* is the rate of charge of the EV battery and $NE_t$ denotes the number of EVs at interval *t* for a parking lot. Furthermore, the equivalent charger capacity of all chargers of EVs is given by Equation ( 18 ). As shown in Equation ( 17 ), the term $SE^{max}$ is equal to $SE_t^{\max} = \sum_{i=1}^{NE_t} SE_i$, where *SE* is the capacity of the EV charger. Finally, the energy consumption requirements of batteries for EVs in a parking lot are represented by Equation ( 19 ). *EC* refers to the overall energy needs of a parking lot, where the energy required for individual EVs will be (1-*SOC*) × *BC*. *SOC* and *BC* introduce the state of charge and battery capacity, respectively. The former means the amount of energy (in %) in the battery after the EV arrives at the parking lot [9]. Thus, *SOC* has a direct relationship with the distance the EV traverse in the electric mode (*L*) and is equal to $(1-L/AER)$; *AER* (all the electrical range) represents the distance the EV moves in the electric mode based on its battery capacity.

5) Technical limits in different networks: The technical limits refer to voltage, pressure, temperature, station power, and line flow. The electrical network index limits including bus voltages, power flows on lines, and power limits of substations are given in ( 20 ) through ( 22 ), respectively [25]. The natural gas network index limits including the amounts of pressure, gas flow, and power generation of the gas grid are stated by Equations ( 23 ) through ( 25 ), respectively [33]. Finally, the district heating network index limits including the temperature, heat power flow, and the power generation of the heat grid are represented by Equations ( 26 ) to ( 28 ), respectively [33].

$$V_e^{\min} \le V_{e,t} \le V_e^{\max} \quad \forall e,t \tag{20}$$

$$(F_{e,j,t}^{p,ele})^2 + (F_{e,j,t}^{q,ele})^2 \le (F_{e,j}^{e,\max})^2 \quad \forall e,j,t \tag{21}$$

$$(P_{e,t}^{ele})^2 + (Q_{e,t}^{ele})^2 \le (S_e^{\max})^2 \quad \forall e,t \tag{22}$$

$$\pi_g^{\min} \le \pi_{g,t} \le \pi_g^{\max} \quad \forall g,t \tag{23}$$

$$-F_{g,j}^{g,\max} \le F_{g,j,t}^{gas} \le F_{g,j}^{g,\max} \quad \forall g,j,t \tag{24}$$

$$0 \le P_{g,t}^{gas} \le P_g^{gas,\max} \quad \forall g,t \tag{25}$$

$$T_h^{\min} \le T_{h,t} \le T_h^{\max} \quad \forall h,t \tag{26}$$

$$-F_{h,j}^{t,\max} \le F_{h,j,t}^{tem} \le F_{h,j}^{t,\max} \quad \forall h,j,t \tag{27}$$

$$0 \le P_{h,t}^{tem} \le P_h^{tem,\max} \quad \forall h,t \tag{28}$$

## B. The equivalent LP problem model

In the original proposed method, Equations ( 1 )-( 28 ) and Constraints ( 4 ), ( 5 ), ( 8 ), ( 13 ), ( 16 ), ( 18 ), ( 21 ), and ( 22 ) are non-linear equations, whereas Constraints ( 4 ) and ( 5 ) are non-convex equations [26]. Hence, the originally proposed method is a non-convex NLP model. Therefore, it is solved by a numerical method that has high computation time [32]. Moreover, this problem fails to reach the global optimal solution because of nonconvex equations [34]. Hence, an equivalent LP model is adopted in the current research for the base problem and it finds the global optimal solution with a low computational time [34].

In the linearization techniques ( 4 ) and ( 5 ), we assume that 1) voltage is $V^{\min} + \sum_{l \in \Phi_l} \Delta V_l$ using the

traditional piecewise linearization approach [26], in which $\Delta V$ < 1 p.u., and 2) the difference between voltage angle is less than 6 degrees or 0.105 rad [26]. Therefore, the terms $V^2$ and $V_eV_j$ are formulated as $(V^{\min})^2 + \sum_{l\in\Phi_l} m_l \Delta V_l$ and $(V^{\min})^2 + V^{\min} \sum_{l\in\Phi_l} \Delta V_{b,l} + V^{\min} \sum_{l\in\Phi_l} \Delta V_{j,l}$, respectively, using the conventional piecewise linearization method [34] and $m$ represents the line slop. Furthermore, $\cos(\theta_{e,t} - \theta_{j,t})$ and $\sin(\theta_{e,t} - \theta_{j,t})$ are converted into 1 and $(\theta_{e,t} - \theta_{j,t})$ as per the second assumption. Thus, the linear equations ( 4 ) and ( 5 ) can be expressed as follows, where $\Delta V\ V^2$ and $\Delta V.(\theta_e - \theta_j)$ are considered zero.

$$F^{p,ele}_{e,j,t} = g_{e,j}\Big(\sum_{l\in\Phi_l}(m_l - V^{\min})\Delta V_{e,t,l} - V^{\min}\Delta V_{j,t,l}\Big) - (V^{\min})^2 b_{e,j}(\theta_{e,t} - \theta_{j,t}) \quad \forall e,j,t \tag{29}$$

$$F^{q,ele}_{e,j,t} = -b_{e,j}\Big(\sum_{l\in\Phi_l}(m_l - V^{\min})\Delta V_{e,t,l} - V^{\min}\Delta V_{j,t,l}\Big) - (V^{\min})^2 g_{e,j}(\theta_{e,t} - \theta_{j,t}) \quad \forall e,j,t \tag{30}$$

Based on the first assumption, i.e. $V = V^{\min} + \sum_{l\in\Phi_l} \Delta V_l$, Equation ( 20 ) is rewritten as follows:

$$0 \le \Delta V_{e,t,l} \le \frac{V_e^{\max} - V_e^{\min}}{N_l} \quad \forall e,t,l \tag{31}$$

$N_l$ denotes the number of the linearization segments in the piecewise method. For linearization of Constraint ( 8 ), it is written as ( 32 ) in the first step, where σ is the auxiliary variable. Moreover, σ is calculated from the equation $(\sigma_{g,j,t})^2 = sign(\pi_{g,t}, \pi_{j,t})(\pi^2_{g,t} - \pi^2_{j,t})$ and converted into a linear equation with the traditional piecewise linearization method [34] as ( 33 )-( 35 ).

$$PL^{gas}_{g,j,t} = sign(\pi_{g,t}, \pi_{j,t})\kappa_{g,j}\sigma_{g,j,t} \tag{32}$$

$$\sum_{l\in\Phi_l} m^{\sigma}_l \Delta\sigma_{g,j,t,l} = sign(\pi_g, \pi_j)\Big(\sum_{l\in\Phi_l} m^{\pi}_l(\Delta\pi_{g,t,l} - \Delta\pi_{j,t,l})\Big) \quad \forall g,j,t \tag{33}$$

$$\sigma_{g,j,t} = \sum_{l\in\Phi_l} \Delta\sigma_{g,j,t,l} \quad \forall g,j,t \tag{34}$$

$$\pi_{g,t} = \pi^{\min}_g + \sum_{l\in\Phi_l} \Delta\pi_{g,t,l} \quad \forall g,t \tag{35}$$

where $m^{\pi}$ and $m^{\sigma}$ are line slop for variables $\pi$ and $\sigma$, respectively. For linearization of ( 16 ), note that $P^{EV}$ and $Q^{EV}$ are positive and negative, respectively, due to Equation ( 17 ) and the inductive property of the electrical network [26]. Hence, terms of $|P^{EV}|$ and $|Q^{EV}|$ are expressed as $P^{EV}$ and $-Q^{EV}$, respectively. Thus, the linear equation for ( 16 ) is as follows:

$$P^{loss}_{e,t} = a^p P^{EV}_{e,t} - a^q Q^{EV}_{e,t} \quad \forall e,t \tag{36}$$

Finally, ( 13 ), ( 18 ), ( 21 ), and ( 22 ) are circular inequalities converted into linear inequality based on [34]. According to [34], the circular plane is approximated to a polygon, the edges of which are straight lines, and the equations are formed by depicting tangents on the circle at different points as ( 37 ). Consequently, the equivalent linear constraints with ( 13 ), ( 18 ), ( 21 ), and ( 22 )are as ( 38 ), ( 39 ), ( 40 ), and ( 41 ), respectively.

$$P \times \cos(\kappa \times \Delta a) + Q \times \sin(\kappa \times \Delta a) \le S^{\max} \quad \forall \Delta a = \frac{360}{n}, \kappa \in \{1, 2, \ldots, n-1\} \tag{37}$$

$$P_{e,t}^{CHP,ele} \cos(\kappa \times \Delta a) + Q_{e,t}^{CHP,ele} \sin(\kappa \times \Delta a) \le S_e^{CHP,e\max} \quad \forall e,t,\kappa \tag{38}$$

$$P_{e,t}^{EV} \cos(\kappa \times \Delta a) + Q_{e,t}^{EV} \sin(\kappa \times \Delta a) \le S_{e,t}^{\max} \quad \forall e,t,\kappa \tag{39}$$

$$F_{e,j,t}^{p,ele} \cos(\kappa \times \Delta a) + F_{e,j,t}^{q,ele} \sin(\kappa \times \Delta a) \le F_{e,j}^{e,\max} \quad \forall e,j,t,\kappa \tag{40}$$

$$P_{e,t}^{ele} \cos(\kappa \times \Delta a) + Q_{e,t}^{ele} \sin(\kappa \times \Delta a) \le S_e^{\max} \quad \forall e,t,\kappa \tag{41}$$

Thus, the suggested LP model will be:

$$\min Total\cos t = \sum_{t\in\Phi_t}\sum_{e\in\Phi_e}^{Electrical\ energy\ \cos t} \rho_t^{ele} P_{e,t}^{ele} + \sum_{t\in\Phi_t}\sum_{g\in\Phi_g}^{Gas\ \ energy\ \ \cos t} \rho^{gas} P_{g,t}^{gas} + \sum_{t\in\Phi_t}\sum_{h\in\Phi_h}^{Heating\ energy\ \cos t} \rho^{tem} P_{h,t}^{tem} \tag{42}$$

Subject to:

(2), (3), (6), (7), (9)-(12), (14), (15), (17), (19), (23)-(36), (38)-(41)

# III. UNCERTAINTY MODEL

## A. Uncertain parameters

In the suggested method, active and reactive power demand ($D^{p,ele}$, $D^{q,ele}$), gas demand ($D^{gas}$), heat demand ($D^{tem}$), electricity price ($\rho^{ele}$), size of EVs charger ($SE^{max}$), rate of charge of batteries ($CR^{max}$), and the energy needs in a parking lot ($EC$) are considered uncertainties. Hence, the matrix of uncertainty is as ( 43 ).

$$u = \left[ D_{e,t}^{p,ele} \; D_{e,t}^{q,ele} \; D_{g,t}^{gas} \; D_{h,t}^{tem} \; \rho_t^{ele} \; CR_{e,t}^{\max} \; SE_{e,t}^{\max} \; EC_e \right] \tag{43}$$

where $u$ introduces the matrix of uncertain parameters.

## B. Point estimate method (PEM) for assessing uncertain parameters

The PEM is a sub-set of the model of probabilities, suitable for modeling uncertainties in the proposed method [35]. In this method, $d$ and $u$ denote deterministic and uncertain input parameters, respectively, and $y$ is the output function of the input parameters expressed as follows:

$$y = f(u, d) \tag{44}$$

In PEM, the expected value and the standard deviation of y are approximately computed based on those of u. If there are n parameters in the matrix or vector of u ($u\tau$, $\tau$ = 1:n), thus, this method uses 2n calculations to obtain the expected value and the variance of y. PEM steps are as follows [35]:

**Step 1:** Compute the placement $\Phi_{\tau,i}$ and probability $\pi_{\tau,i}$ based on (45) and (48), respectively.

$$\Phi_{\tau,i} = \frac{M_3(u_\tau)}{2\sigma_{u_\tau}^3} + (-1)^{i+1}\sqrt{S + \frac{1}{2}\left(\frac{M_3(u_\tau)}{\sigma_{u_\tau}^3}\right)^2}; \tau = 1:n, i = 1,2 \quad (45)$$

$$\pi_{\tau,i} = (-1)^i \frac{\Phi_{\tau,3-i}}{2S\sqrt{S + \frac{1}{2}\left(\frac{M_3(u_\tau)}{\sigma_{u_\tau}^3}\right)^2}}; \tau = 1:n, i = 1,2 \quad (46)$$

where $\tau$ is the indices of uncertain parameters, $\sigma_{u_\tau}$ is the standard deviation of $u_\tau$, and $M_3(u_\tau)$ is the third moment of $u_\tau$ computed as:

$$M_3(u_\tau) = E\left[(u_\tau - \mu_{u_\tau})^3\right] \quad \tau = 1:n \quad (47)$$

$E$ is the expected value and $\mu_{u_\tau}$ is the average of $u_\tau$.

**Step 2:** Determine $u_{\tau,i}$ as follows:

$$u_{\tau,i} = \mu_{u_\tau} + \Phi_{\tau,i}\sigma_{u_\tau} \quad \tau = 1:n, i = 1,2 \quad (48)$$

**Step 3:** Compute the expected value and variance of $y$ using ( 49 ) and ( 50 ), respectively. If $\tau = p$, the uncertain parameter p in vector u should be replaced with $u_{\tau,i}$. Other parameters of u can be identified with its average value.

$$E(y) = \sum_{\tau=1}^{n}\sum_{i=1}^{2}\pi_{\tau,i} f(d, \mu_{u_1}, \mu_{u_2}, ..., u_{\tau,i}, ..., \mu_{u_s}) \quad (49)$$

$$E(y^2) = \sum_{\tau=1}^{n}\sum_{i=1}^{2}\pi_{\tau,i} f^2(d, \mu_{u_1}, \mu_{u_2}, ..., u_{\tau,i}, ..., \mu_{u_s}) \quad (50)$$

**Step 4:** Compute the average value and standard deviation of $y$ using ( 51 ) and ( 52 ), respectively.

$$\mu_y = E(y) \quad (51)$$

$$\sigma_y = \sqrt{E(y^2) - E^2(y)} \quad (52)$$

Figure 2. depicts the flowchart of the proposed method.

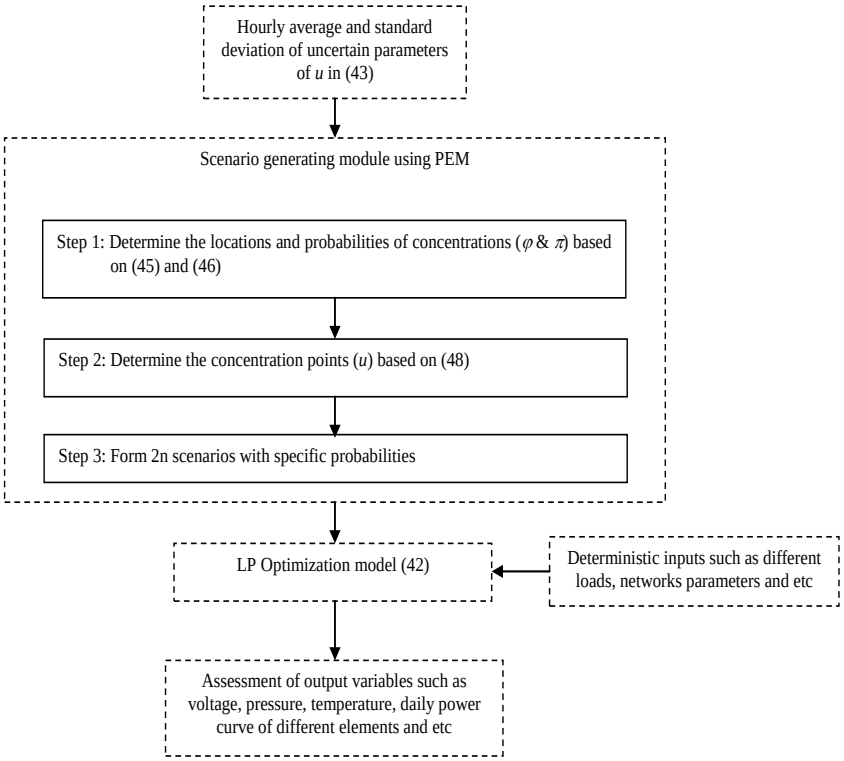


**Figure 2.** Complete procedure of the suggested probabilistic linear programming (PLP) model using PEM

# IV. NUMERICAL STUDIES

## A. Case study

The suggested approach is used for nine electrical buses, four gas nodes, and nine heat nodes with seven EHs, as shown in Figure 3. In this network, there are four electrical stations in buses 1, 2, 3, and 7 with the capacity of 7, 5, 4, and 4 MVA. Also, gas and heat stations are 8 and 3 MW, respectively. The base power for all the networks is selected as 1 MW. The base voltage, pressure, and temperature values are 1 kV, 10 bar, and 100°C, respectively, with similar limits in the range of [0.9, 1.1] p.u. Specifications of electrical lines together with gas and heat lines are described in [33]. The mean value of loads at 20:00 is shown in Table 2 [33]. The amount of load at other hours of the day can be obtained by multiplying the daily load factor curve by the load at 20:00. The load factor curves are presented in Figure 4(a) [15]. The standard deviation of different loads is selected similarly and equal to 0.05 p.u. In addition, the mean and standard deviation of the electrical energy price is given in [35]. Moreover, the prices of energy for gas and heat (biomass) stations are assumed 14 and 8 [33] $/MWh, respectively.

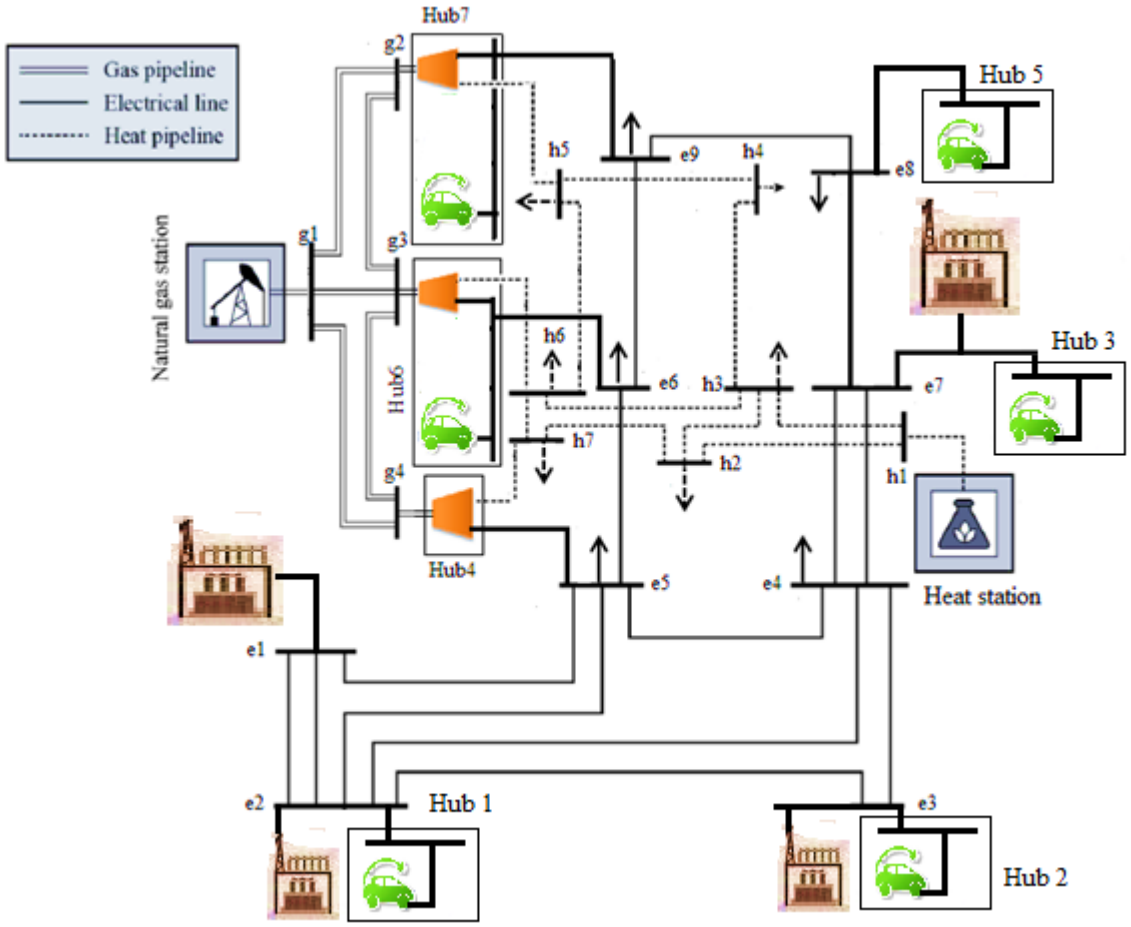


**Figure 3**.The multicarrier energy system

**Table 2**. Electrical and heating loads at the hour 20:00 (p.u.) [33]

| Electrical network | | | District heating network | |
|---|---|---|---|---|
| Bus | $PD^{ele}$ | $QD^{ele}$ | Bus | $PD^{tem}$ |
| 1 | 0.5 | 0.3 | 1 | 0 |
| 2 | 0.8 | 0.4 | 2 | 0.8 |
| 3 | 0 | 0 | 3 | 0.7 |
| 4 | 0.9 | 0.3 | 4 | 0.9 |
| 5 | 0.7 | 0.5 | 5 | 0.6 |
| 6 | 1 | 0.2 | 6 | 0.5 |
| 7 | 0.6 | 0.4 | 7 | 0.7 |
| 8 | 0.8 | 0.5 | | |
| 9 | 0.7 | 0.3 | | |

This network has seven EHs. EHs 1, 2, 3, and 5 contain EVs and are placed in electrical buses 2, 3, 7, and 8. EH 4 contains only CHP and is placed in electrical bus 5, gas node 4, and heat node 7. EHs 6 and 7 both contain CHP units and EVs parking lots and are placed in electrical buses 6 and 9, i.e. the gas nodes 3 and 2 as well as the heating nodes 6 and 5. Within the given EHs, the maximum capacity of CHP units in the gas, electricity, and heat sectors is 2.5, 1, and 1 p.u. with an efficiency of 80% [33]. There are 200 EVs in each parking lot. Figure 4(b) shows the mean and standard deviation values of $NE_t$. Characteristics of EVs like battery capacity, state of charge, and other parameters can be found in [26]. Finally, the standard deviation of *EC* is selected as 0.1 p.u. and the starting time of the simulation is set to 10:00 according to Equation ( 19 ).

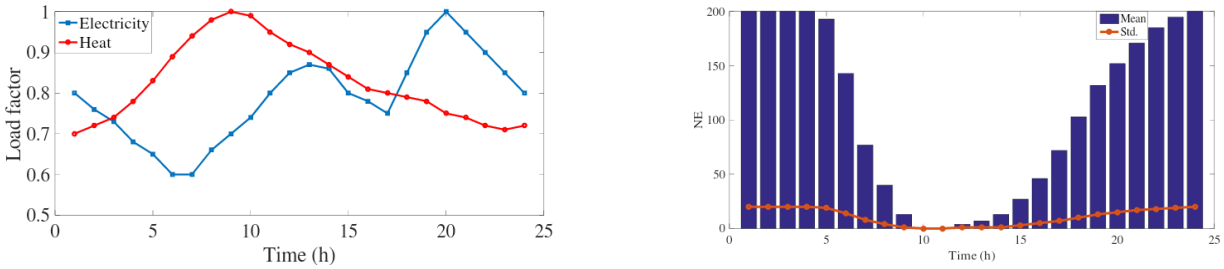


(a) (b)

**Figure 4**. Daily mean and standard deviation values of NE

## B. Simulation results

Simulations are carried out using GAMS 23.5.2 and NLP and LP models are solved by CONOPT and CPLEX solvers, respectively [36]. It is noted that one of the solvers of the NLP method in GAMS software is CONOPT which is based on the Karish-Kuhn-Tucker method and its solving approach is according to the numerical method such as the Jacobian matrix in the Newton Raphson method. More details of this method are presented in [37]. Also, the CPLEX is a suitable solver for the LP method, which is based on the simplex approach [38].

1) Comparing the suggested NLP and LP models: *Results* related to deterministic LP and NLP models are presented, where uncertainty values are equal to their mean values. Moreover, the number of linearization segments in the piecewise method and circular constraints is 5 and 30, respectively. Table 3 tabulates the results related to the presented NLP and LP models for different variables. As is observed, the calculation error for the LP model in comparison with the NLP model is about 2.5%, 0.5%, 0.35%, 0.9%, 0.1%, 0%, and 0 for active and reactive power, voltage magnitude, voltage angle, gas power, pressure, heating power, and temperature, respectively. Power flow equations for the district heating network, ( 9 )-( 10 ), are the same for the two models; hence, the calculation error for the district heating network indices or variables is equal to 0. Hence, the total cost for the proposed method in the NLP model is equal to \$6512.54; but it is \$6368.32 for the LP model which includes a deviation of 2.21% ((6512.54 – 6368.32)/6512.54) compared with NLP method. Moreover, the computation time in the LP model is much less than that in the NLP model. Therefore, the LP model can be used instead of the NLP model as the computation speed of the former is significantly faster than the latter and leads to a lower computational error. Therefore, the results demonstrate desirable benefits of the second contribution, where the linearized model achieves the optimal solution at low computational error and time.

**Table 3**. Results of LP and NLP models for hour 20:00

| Parameter | NLP | LP | Deviation percent |
|---|---|---|---|
| Total station active power (pu) | 4.4668 | 4.246 | 2.52% |
| Total station reactive power (pu) | 2.9712 | 2.9 | 2.47% |
| Total station gas power (pu) | 3.5315 | 3.5 | 0.9% |
| Total station heating power (pu) | 2.204 | 2.204 | 0 |
| Mean of voltage magnitude (pu) | 0.9778 | 0.973 | 0.5% |
| Mean of voltage angle (pu) | 0.004014 | 0.004 | 0.35% |
| Mean of pressure (pu) | 0.927 | 0.926 | 0.1% |
| Mean of temperature (pu) | 0.933 | 0.933 | 0 |
| Objective function (\$) | 6512.54 | 6368.32 | 2.21% |
| Calculation time (s) | 510 | 22 | 95.68% |

2) Assessment of energy hub elements operation: Figure 5 and 6 show the expected results of this

section in the form of daily power curves of different elements of MES. In these figures, the horizontal axis is simulation time which refers to hours 10:00 to 24:00 for today and 1:00 to 9:00 on the next day. Figure 5 depicts the daily active and reactive power curves of all EVs. As is seen from Figure 5(a), EVs are charged during off-peak hours of electricity consumption, i.e. from 1:00 to 7:00, so that the objective function minimizes the electricity price. The electricity price is 16, 24, and 30 $/MWh during 1:00-7:00, ٨:٠٠-١٦:٠٠ as well as ٢٣:٠٠-٢٤:٠٠, and ١٧:٠٠-٢٢:٠٠ [35]. Thus, in periods 1:00 to 7:00, it is lower than other simulation hours according to [35]. Hence, to obtain low charging costs and minimize the energy cost, all EVs receive high power from CHPs or electrical networks to supply their requirement consumption energy in this period. As is seen in Figure 5(b), EVs inject large amounts of reactive power into the grid between 1:00 and 7:00. The reason is that the electricity demand is high during this interval as EVs are charged and, hence, the voltage drop will be high. Thus, EVs inject reactive power into the electricity grid to compensate for voltage drops. Moreover, at hours 10:00-24:00 today and 8:00-9:00 on the next day, EVs do not absorb active power from the electricity grid due to higher electricity energy prices at these hours than the period of 1:00-7:00 on the next day [35] and minimizing the energy cost. Also, they do not inject reactive power into the network during these intervals, because the power loss of EV chargers will be increased by increasing the EV's reactive power injection based on Equation ( 16 ). Hence, the electrical energy cost is increased in these periods if EVs inject reactive power into the network.

Furthermore, references [23] investigate active (charge and discharge)/(charge) and reactive power management of a distribution system including only EVs parking lot. In [23], EVs were charged in the period 12:00-16:00 to provide EVs discharging energy in the period 18:00-22:00 and they were charged in the period 1:00-7:00 to obtain their requirement consumption energy in the trip. Hence, the number of charge and discharge cycles of EV batteries in [23] was greater than the one in this paper; in [23], EV battery lifetime was reduced with respect to the work in this paper. Also, in [23], EVs injected high reactive power into the distribution system during the whole simulation time. This case increased the switching number in the EV charger; thus, in [23], the EV charger lifetime was reduced compared with the work in this paper. Therefore, this demonstrates the advantages of the first proposed contribution; in which the coordination scheme of EVs and CHP as an EH framework can improve EV battery and charger lifetime as well as operation cost.

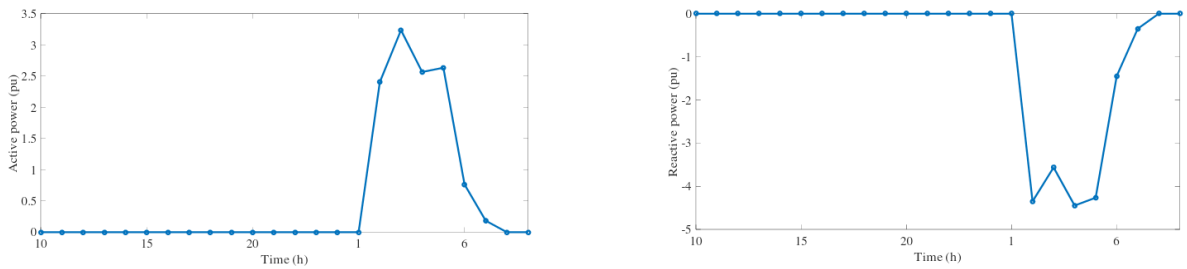


(a) (b)

**Figure 5**. Daily curves of the total power of EVs, a) active power, and b) reactive power

Figure 6 depicts the daily active, reactive, heating, and gas power curves of CHPs. As is observed in Figure 6(a), all CHPs inject high active power into the electricity grid during 10:00-00:00 to supply the electrical network load demand which is high in this period according to Figure 4(a) and in period 1:00-7:00 to provide energy demand of EVs and the electrical network. Also, CHPs inject reactive power into the electrical network between 0.25 and 1.2 p.u. at all simulation hours. Note that the scheduling of CHPs active and reactive power aims to minimize the electrical energy price and regulate voltage based on objective function ( 1 ) and Equations ( 2 )-( 5 ). In addition, according to Figure 6(c), CHPs inject heat power into the heating grid according to the demand of this network, so that they inject high/low heating

power into this network in periods 10:00-15:00 and 6:00-9:00/16:00-5:00 to supply high/low heating load demand in the heating network based on Figure 4(a). Moreover, this could be attributed to the point that the heat power of CHP is 1 p.u., while its active power is 0. Thus, the gas power ( 11 ) will be 1.25 p.u. and the energy cost is 17.5$ (1.25*14). However, should the heating power be injected into the heat grid through heating stations, the energy cost will be 8$ (1*8). So, CHPs inject low heat power into the heat grid for more hours. In addition, the gas network provides the input gas power for all CHPs based on Figure 3 and the daily gas power curve of all the CHPs is similar to Figure 6(d) which is constant at all hours. Since the power depends on active and heating power in CHPs according to Equation ( 11 ), as shown in Figure 6(a) and 6(c), it is constant at all hours.

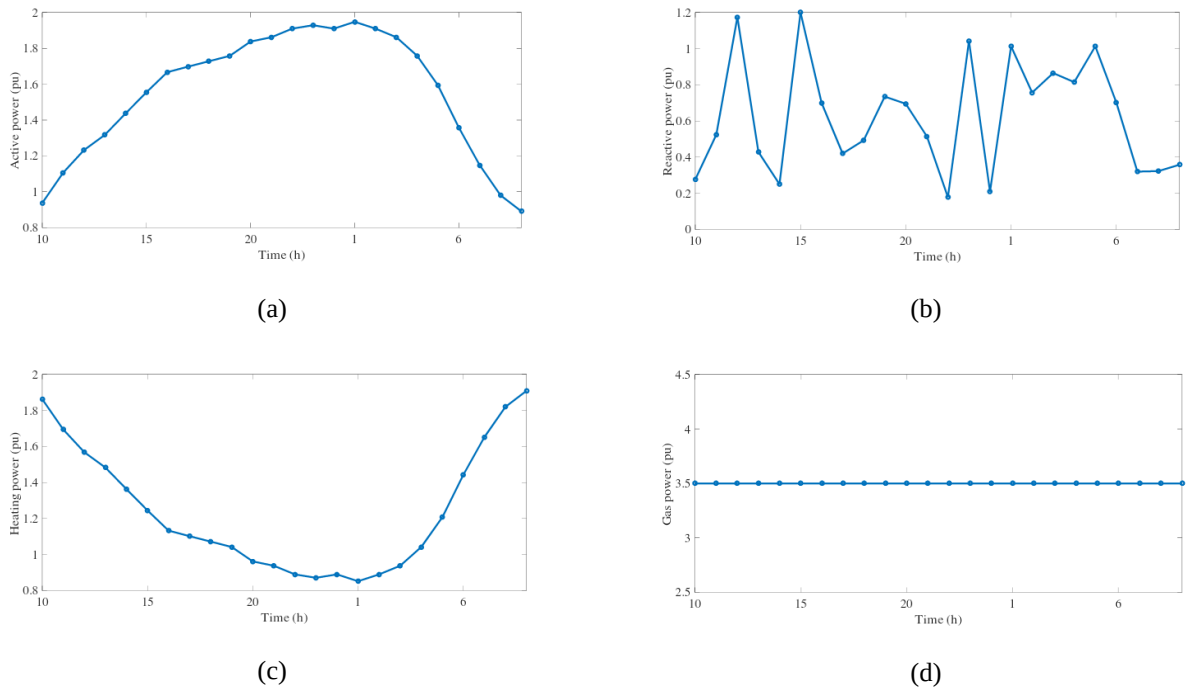


**Figure 6**. Daily CHP power curves of different energy sectors, a) active power, b) reactive power, c) heating power, d) gas power

3) Assessment of different network indices: Figure 7 and 8 show the average results. As one can observe from Figure 7, daily active, reactive, gas, and heat power curves in different networks (electricity, gas, and heat) are presented. According to Table 2, the total active power is 5.9 p.u. at 20:00 and the total reactive power is 2.9 p.u. at 20:00. However, according to Figure 7(a) and 7(b), the total active and reactive power is 4.3 and 2.3 p.u. at 20:00. To elucidate, the station power of the electrical grid in the presence of MES is reduced in periods 1:00-24:00 today and 8:00-9:00 on the next day with respect to the suggested method in the absence of MES, because CHPs inject the active and reactive powers into this network according to Figure 6(a) and 6(b). But, it increases in period 1:00-7:00 in comparison with the case without MES due to the high absorbing active power by EVs in this period based on Figure 5(a). This statement can also be regarded in the heat grid as is seen in Figure 7(c) so that the heat station provides a high value of heating load demand during the whole simulation time. Since the heat energy price is less than the gas price as per Section IV.A, the high value of heating energy is supplied by heat station compared with CHPs which converts gas power into electricity and heating power regarding Figure 6(c) and 7(c). Moreover, the gas demand of the test grid is 0; hence, the supplied gas power equals gas power in the gas sector of CHPs in MES based on Figure 6(d). As a result, the station gas power

increases in the case of the proposed method in comparison to the case where the method does not use the MES.

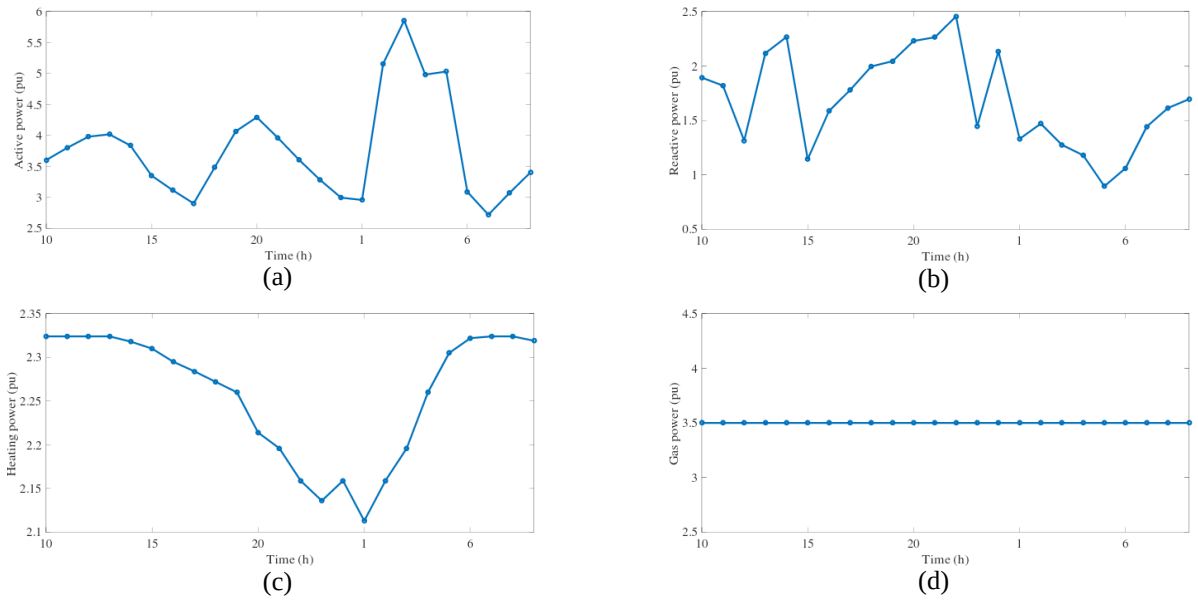


**Figure 7**. Daily curves of the station power for different networks, a) active power, b) reactive power, c) heating power, and d) gas power.

The profiles of voltage in electrical buses, pressure in gas nodes, and temperature in the heating nodes at hour 20:00 are shown in Figure 8, where the values of voltage, pressure, and temperature are between [0.9, 1.1] p.u. Further, based on Figure 8(a), the voltage has a high magnitude in bus 2, but a low value in bus 9. The reason is that the generation capacity of bus 9 is 0 and the distance between this bus and the electrical reference bus is higher than the rest of the buses. So, the voltage amplitude of bus 9 is smaller than that of the rest of the buses. Nevertheless, the power generation of bus 2 is high and large power is injected into the grid. Consequently, the voltage of bus 2 is greater than that of the rest of the buses. According to Figure 8(b), the pressure of node 3 is more than the pressure of nodes 2 and 4. In addition, the temperature of node 2 is more than that of nodes 3-7 based on Figure 8(c). This is because the distance between node 3 and the natural gas reference node (node 1) is lower than nodes 2 and 4. Hence, the pipeline constant between nodes 1 and 3 as well as the pressure drop of node 3 is low. Moreover, $c \times \dot{m}$ between node 1 of the district heating network and node 2 is lower than other nodes. Therefore, node 2 has a higher temperature than nodes 3-7.

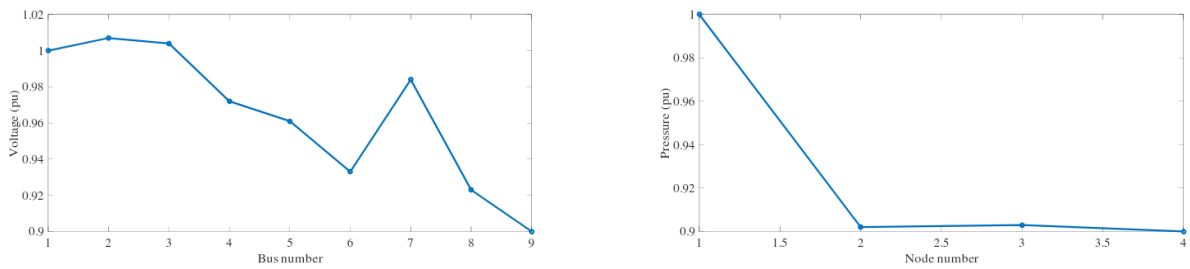

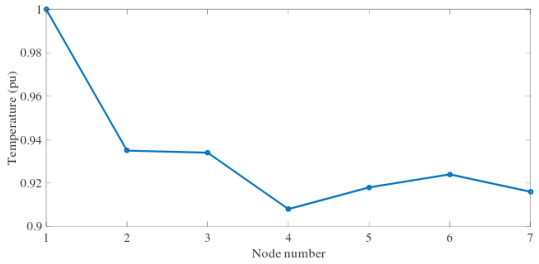


(c)

**Figure 8.** Index profiles for various grids during hour 20:00, a) voltage, b) pressure, and c) temperature

Table IV provides the expected value of different energy costs (refer to Figure 7). According to this table, the energy cost of the electrical network is the highest, while the district heating network has the lowest cost. The reason is a higher price of electricity and a lower price of heat. In addition, the table lists different energy costs for the deterministic model. Accordingly, the electrical energy cost in the PEM-based stochastic method is higher than the deterministic model by about 4.64% ((5022.089 – 4799.43)/ 4799.43) due to considering uncertain parameters. This deviation for gas and heating energy costs is equal to 2.04% and 4.16%. Hence, the cost difference between stochastic and deterministic methods is equal to 263.531 $ (6631.851 – 6368.32) due to considering uncertain parameters. Therefore, the proposed strategy pays 263.531 $ more to networks or market operators in the stochastic model than in the deterministic model to remove the contingency arising from the proposed uncertainties. Also, the difference between stochastic and deterministic methods in the scenario-based stochastic programming (SBSP) technique [39] equals 266.89 $ arising from considering the uncertainties associated with energy demand, price of energy, and EVs demand. As per Table 4, the approach in [39] obtains the optimal solution at 86 sec, while the PEM approach achieves this optimal point at 43 sec. This statement hold as the number of scenarios in the SBSP is greater than that in the PEM approach. Finally, this case demonstrates the benefits of the proposed third contribution.

**Table 4**. The value of different energy cost

| Model | Deterministic model | Scenario-based stochastic programming [39] | Stochastic based on PEM |
|---|---|---|---|
| Calculation time (second) | 22 | 86 | 43 |
| Electricity energy cost ($) | 4799.43 | 5024.19 | 5022.089 |
| Gas energy cost ($) | 1152.48 | 1177.1 | 1176 |
| Heating energy cost ($)) | 416.41 | 433.92 | 433.762 |
| Total energy cost ($) | 6368.32 | 6635.21 | 6631.851 |
| Difference between stochastic and deterministic models ($) | | 266.89 | 263.531 |

## V. CONCLUSIONS

This study presented a model for MES management considering EVs and CHP units. In this study, electricity and gas were assumed as the inputs to the MES, whereas electricity and heat were the outputs of the MES. The considered model was structured in the form of an optimization problem, where the objective function minimizes the energy cost in MES. The constraints included power flow equations and limitation of technical indices in MES, constraints of EVs parking lot, and CHPs. Then, the equivalent LP model with base formulation achieved the global optimal solution. Moreover, electricity, gas, and heat demand, price of electricity, and different variables of EVs were taken into account as uncertainties. Hence, the point estimate method was employed and uncertainties were modeled. As per the obtained results, the suggested LP model obtains results close to the global optimal solution while resulting in a

lower computation time and error. Moreover, it was observed that the presence of energy hubs including CHP units and EVs in various networks reduced the demand during peak hours using energy management of hub devices. To put it simply, according to the suggested energy management of the MESs, EVs were charged in a low electricity load period to obtain low energy or charging cost; also, they injected high reactive power in this period to regulate the voltage in the electrical network. Also, all CHPs injected optimal active, reactive, and heating powers into the electrical and heating networks according to MESs and networks' demands. Therefore, the indices of different networks were improved using the power and energy management of MESs and it was predicted that the MESs or EHs can improve the operation, flexibility, reliability, security, and other indicators of different networks using the proposed energy management method.

Modeling the proposed scheme is in accordance with improving the operation of energy networks. Nonetheless, with proper management of the hubs' energy, they can participate in the energy market and ancillary services and benefit from them financially. This topic is suggested for future work. In addition, the energy hub is distributed at consumption points. Therefore, with proper energy management, it is predicted that in the event of a fault in energy networks, hubs could compensate for a percentage of consumer interruptions and improve the reliability of the networks. This is also suggested as future work.

The data and its supplementary material that supports the findings of this study are available.

## References

[1] O. Dzobo, X. Xia, "Optimal operation of smart multi-energy hub systems incorporating energy hub coordination and demand response strategy," *Journal of Renewable and Sustainable Energy*, vol. 9, pp. 045501, 2017.

[2] A. Reza, T.N. Malik, "Bogas supported bi-level macro energy hub management system for residential customers," *Journal of Renewable and Sustainable Energy*, vol. 10, pp. 025501, 2018.

[3] M.S.Nazar, M.R. Haghifam, "Multiobjective electric distribution system expansion planning using hybrid energy hub concept," *Electric Power Systems Research*, vol. 79, pp. 899-911, 2009.

[4] T. Krause, G.Andersson, K. Fröhlich, A. Vaccaro,"Multipleenergy carriers: modeling of production, delivery, and consumption," *IEEE Proceedings*, vol. 99, pp. 15-27, 2011.

[5] M. Geidl, Integrated modeling and optimization of multi-carrier energy systems, *PhD thesis*, 2007.

[6] M. Hou, Y. Zhao, X. Ge, "Optimal scheduling of the plug-in electric vehicles aggregator energy and regulation services based on grid to vehicle," *International Transactions on Electrical Energy Systems*, vol. 27, pp. 1-12, 2017.

[7] R.C. Leou, C.L. Su, and C.N. Lu, "Stochastic analyses of electric vehicle charging impacts on distribution network," *IEEE Trans. Power Syst.*, vol. 29, no. 3, pp. 1055-1063, May 2013.

[8] S. Pirouzi, M.A. Latify, and G.R. Yousefi, "Investigation on reactive power support capability of PEVs in distribution network operation," *23rd Iranian Conference on Electrical Engineering (ICEE)*, May 2015.

[9] S. Shafiee, M. Fotuhi-Firuzabad, and M. Rastegar,, "Investigating the impacts of plug-in hybrid electric vehicles on power distribution systems," *IEEE Transactions on Smart Grid.*, vol. 4, no. 3, pp. 1351-1360, 2013.

[10] A. Rabiee, H. Farahani, M. Khalili, J.Aghaei, K. Muttaqi, "Integration of plug-in electric vehicles into microgrids as energy and reactive power providers in market environment," *IEEE Transactions on Industrial Informatics*, DOI: 10.1109/TII.2016.2569438, *Article in press*, 2016.

[11] M. Moeini-Aghtaie, A. Abbaspour, M. Fotuhi-Firuzabad,,E. Hajipour, "A decomposed solution to multiple-energy carriers optimal power flow," *IEEE Transactions on Power Systems*, vol. 29, pp. 707-716, 2014.

[12] M. La Scala, A. Vaccaro, A.F. Zobaa, "A goal programming methodology for multiobjective optimization of distributed energy hubs operation," *Applied Thermal Engineering*, vol. 71, pp. 658-666, 10/22/ 2014.
[13] A. Najafi, H. Falaghi, J. Contreras, and M. Ramezani, "Medium-term energy hub management subject to electricity price and wind uncertainty," *Applied Energy*, vol. 168, pp. 418-433, 2016.
[14] A. Najafi, F. H, J. Contreras, and M. Ramezani, "A Stochastic Bilevel Model for the Energy Hub Manager Problem," *IEEE Transactions on Smart Grid*, vol. 26, no. 3, pp. 1-11, 2016.
[15] A.S. Haghighi, A.R. Seifi, and T. Niknam, "A modified teaching–learning based optimization for multi-objective optimal power flow problem," *Energy Conversion and Management*, vol. 77, pp. 597-607, 2014.
[16] A. Shabanpour-Haghighi and A. R. Seifi, "Multi-objective operation management of a multi-carrier energy system," *Energy*, vol. 88, pp. 430-442, 2015.
[17] S. D. Beigvanda, H. Abdia, M. L. Scalab, "Economic dispatch of multiple energy carriers", *Energy*, Volume. 138, Pages 861-872, 2017.
[18] S. D. Beigvanda, H. Abdia, M. L. Scalab, "A general model for energy hub economic dispatch", *Applied Energy*, Volume 190, Pages 1090-1111, 2017.
[19] M. Aslinezhad, A. Malekijavan, H. Zafarani, "Reliability-based operation in Energy Hubs with several energy networks," International Journal of Industrial Electronics Control Optimization, 2021.
[20] X. Luo, and K.W. Chan, "Real-time scheduling of electric vehicles charging in low-voltage residential distribution systems to minimise power losses and improve voltage profile," *IET Generation, Transmission and Distribution*, vol.8, no.3, pp.516-529, 2014.
[21] F. Milano, and O. Hersent, "Optimal load management with inclusion of electric vehicles and distributed energy resources," *IEEE Transactions on Smart Grid*, vol. 5, no. 2, pp. 662-672, March 2014.
[22] M.C. Kisacikoglu, M. Kesler, and L.M. Tolbert, "Single-phase on-board bidirectional PEV charger for V2G reactive power operation," *IEEE Transactions on Smart Grid*, vol. 6, pp. 767-775, 2015.
[23] S. Pirouzi, J. Aghaei, T. Niknam, H. Farahmand, and M. Korpås, "Proactive operation of electric vehicles in harmonic polluted smart distribution networks," *IET Generation, Transmission and distribution*, vol. 12, pp. 967-975, 2018.
[24] S. Pirouzi, J. Aghaei, M. Shafie-khah, G.J. Osório, J.P.S. Catalão, "Evaluating the security of electrical energy distribution networks in the presence of electric vehicles," in *Proc. PowerTechConf, IEEE Manchester*, pp. 1-6, 2017.
[25] S. Pirouzi, J. Aghaei, "Modeling of electric vehicles contributions in voltage security of smart distribution networks," *SIMULATION: Transactions of the Society for Modeling and Simulation International*, (accepted), 2018.
[26] S. Pirouzi, J. Aghaei, V. Vahidinasab, T. Niknam, and A. Khodaei, "Robust linear architecture for active/reactive power scheduling of EV integrated smart distribution networks," *Electric Power System Research*, vol. 155, pp. 8-20, 2018.
[27] M.A. Norouzi, and et al., "Bi-level fuzzy stochastic-robust model for flexibility valorizing of renewable networked microgrids," *Sustainable Energy, Grids and Networks*, vol. 31, pp. 100684, 2022.
[28] A.R. Azarhooshang, S. Pirouzi, M. Ghadamyari, "Two-stage Framework for Microgrids Energy Management Considering Demand Response Program and Compressed Air Energy Storages under Uncertainties," *International Journal of Smart Electrical Engineering*, vol. 11, no. 3, pp. 149-162, 2022.
[29] M.A. Norouzi, and et al., "Flexibility pricing of integrated unit of electric spring and EVs parking in microgrids," *Energy*, vol. 239, pp. 122080, 2022.

[30] B. Kandpal, P. Pareek, A. Verma, “A robust day-ahead scheduling strategy for EV charging stations in unbalanced distribution grid,” *Energy*, vol. 249, pp. 123737, 2022.
[31] R. Hu, W. Wang, X. Wu, Z. Chen, L. Jing, W. Ma, G. Zeng, “Coordinated active and reactive power control for distribution networks with high penetrations of photovoltaic systems,” Solar *Energy*, vol. 231, pp. 809-827, 2022.
[32] S. Pirouzi, J. Aghaei, M.A. Latify, G.R. Yousefi, and G. Mokryani, “A robust optimization approach for active and reactive power management in smart distribution networks using electric vehicles,” *IEEE System Journal*, 2017.
[33] A. Shabanpour-Haghighi and A. R. Seifi, “Energy Flow Optimization in Multicarrier Systems,”*IEEE Transactions on Industrial Informatics*, vol. 11, pp. 1067-1077, 2015.
[34] S. Pirouzi, J. Aghaei, T. Niknam, M. Shafie-khah, V.Vahidinasab, and J.P.S. Catalão, “Two alternative robust optimization models for flexible power management of electric vehicles in distribution networks,” *Energy*, vol. 141, pp. 635-651, 2017.
[35] A. Shayegan-Rad, A. Badri, A. Zangeneh, “Day-ahead scheduling of virtual power plant in joint energy and regulation reserve markets under uncertainties,” *Energy*, vol. 121, pp. 114-125, 2017.
[36] Generalized Algebraic Modeling Systems (GAMS). [Online]. Available: http://www.gams.com.
[37] GAMS/CONOPT. [Online]. Available: https://www.gams.com/latest/docs/S_CONOPT.html.
[38] GAMS/CPLEX. [Online]. Available: https://www.gams.com/latest/docs/S_CPLEX.html.
[39] J. Aghaei, M. Barani, M. Shafie-khah, A. A. Sánchez de la Nieta and J. P. S. Catalão, "Risk-Constrained Offering Strategy for Aggregated Hybrid Power Plant Including Wind Power Producer and Demand Response Provider," in *IEEE Transactions on Sustainable Energy*, vol. 7, no. 2, pp. 513-525, April 2016.